

# Design of On-board Power Supply for Tether Drone Applications

Taewan Kim<sup>1</sup>, Jinri Kim<sup>1</sup>, and Se-Kyo Chung<sup>2</sup>

<sup>1</sup> Dept. of Electrical & Electronic Engineering, Graduate School, Gyeongsang National University, Jinju, Korea

<sup>2</sup> Dept. of Control & Instrumentation Engineering, Gyeongsang National University, Jinju, Korea

**Abstract-** This paper presents the design of an on-board power supply for the tether drone system used in commercial and military applications. The power supply is crucial for delivering DC power to the propulsion and control systems of the tethered drone. This paper proposes an interleaved LLC resonant converter as the main topology and presents the design and implementation of the converter and control circuits. The integrated magnetic design of the transformer and inductor is also proposed to improve the power density of the converter. The proposed techniques were applied to a 1.6kW converter with input/output voltages of 400V/50V, and experimental results are provided to verify the design of the proposed scheme.

**Index Terms**—Tether drone, Power supply, LLC resonant converter, Interleaved control.

## I. INTRODUCTION

A tether drone is a wired powering drone and is used for the applications requiring a long flight time such as the traffic monitoring, mobile telecom station and surveillance [1]. Recently, as extending the application area of the tether drone, the need for increasing the payload is also grown. Because of this, the design of the power supply system is a critical issue in the tether drone systems [2-4]. The power supply system of the tether drone consists of the ground AC-DC and on-board DC-DC converters as shown in Fig. 1.

The ground AC-DC power supply generates the high voltage DC power and supplies it to the power cable tethered to the drone. The high voltage of 300~800VDC should be required to reduce the weight of the long power cable. The on-board DC-DC converter is fitted on the drone and delivers the low voltage DC power to the

propulsion and control systems. The small size and light weight are crucial for the on-board equipment of aerial systems, and thus the high-power density is an essential requirement of the on-board power supply for the tether drone systems [4]. An interleaved LLC resonant converter can be considered as a possible solution for the main DC-DC converter to satisfy this requirement. The interleaved technique provides the advantage of reducing the size of the passive components [5]-[9]. This paper is focused on the design of the interleaved LLC resonant converter as the main DC-DC converter of the on-board power supply.

The architecture of the on-board power supply is first discussed. The design and implementation of the power circuit, controller and magnetic components are presented. The experimental results for the prototype on-board power supply with a power rating of 1.6kW are provided to verify the effectiveness of the proposed scheme.

## II. DESIGN OF ON-BOARD POWER SUPPLY

### A. Structure of on-board power supply

The structure of the on-board power supply for the tether drone is shown in Fig. 2, which consists of the main DC-DC converter, auxiliary DC-DC converter and power source swapping circuit.

The main DC-DC converter downs the input voltage of 400VDC supplied from the power cable to the low DC voltage of 50VDC used for the bus voltage and driving the electric propulsion motors. The auxiliary converter is for the control electronics and a synchronous buck converter with the input and output voltages of 50VDC and 12VDC, respectively, is used. The power source swapping circuit



Fig. 1. Power supply system for tether drone.

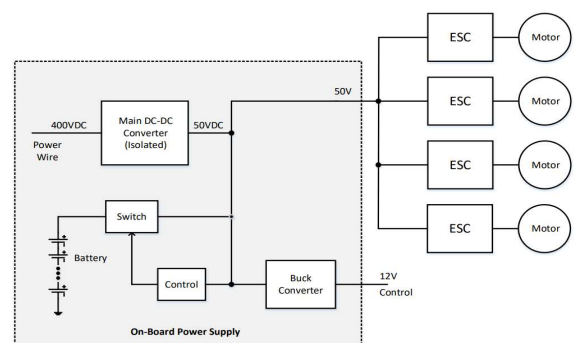


Fig. 2. Structure of on-board power supply for tether drone.

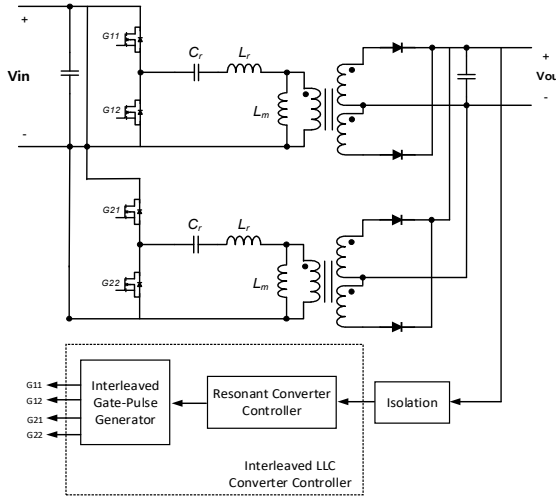


Fig. 3. Two-phase interleaved LLC resonant converter

changes the power source from the cable power to the on-board battery when the power source through the cable is failed.

This paper is focused on the design of the main DC-DC converter which is a dominant element to determine the power density of the on-board power supply.

The two-phase interleaved LLC resonant converter is used in this paper as the main DC-DC converter as shown in Fig. 3. The main issues considered in this paper are the design of the interleaved resonant controller and size reduction of the magnetic components, which will be discussed in the next sections.

#### B. Design of interleaved LLC resonant converter

The interleaved LLC resonant converter considered in this paper has two half-bridge converter modules as shown in Fig. 3. The power rating and input/output voltages for the power stage of each converters are given as:  $P_o=800W$  ( $\times 2$ ),  $V_{in}=400V$ ,  $V_o=50V$ . The design of each half-bridge LLC resonant converter is provided in literatures [10], [11].

First, the turn ratio of the transformer can be determined as follows.

$$n = \frac{N_1}{N_2} = M_g \cdot \frac{V_{in}/2}{V_o} \quad (1)$$

Since the winding ratio is calculated as 4 for gain =1, it is set as  $n=4$ , and the gain is  $M_g=1.0$ . The inductance ratio  $L_n=L_m/L_r$  and the quality factor  $Q_e$  are determined as  $L_n=5.5$  and  $Q_e=0.45$  respectively, using the gain and quality factor curves.

The equivalent load resistance  $R_e$  can be calculated as follows.

$$R_e = \frac{8n^2}{\pi^2} \cdot \frac{V_o}{I_o} \quad (2)$$

In the case of load current =16A (800W) =43.2, the resonance capacitance and inductance are calculated as follows:

$$C_r = \frac{1}{2\pi Q_e f_0 R_e} \quad (3)$$

$$L_r = \frac{1}{(2\pi f_0)^2 C_r} \quad (4)$$

where,  $f_0$  denotes the resonant frequency. The resonant capacitance and inductance are calculated as  $C_r=53.4nF$  and  $L_r=20.2uH$  from equations (3) and (4). The resonant frequency is  $f_0=153$  kHz and the magnetizing inductance is calculated as  $L_m = 111uH$ . The parameters of the converter designed based on the calculated values are shown in Table 1. Fig. 4 shows the gain curves of the designed converter for 20% to 100% load conditions.

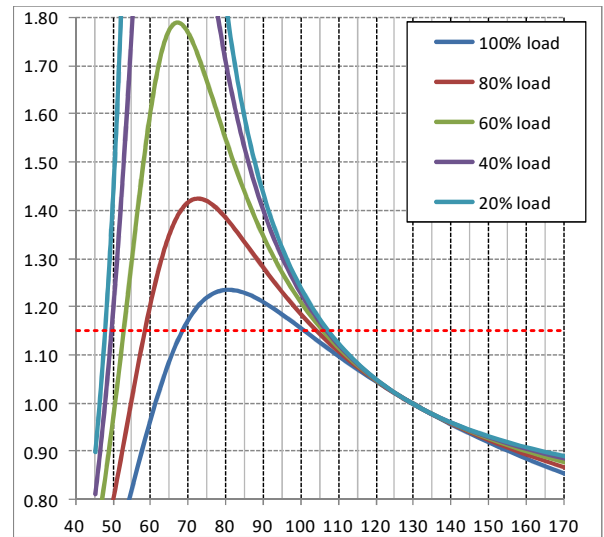


Fig. 4. Gain curves of the designed converter.

TABLE I  
PARAMETERS OF DESIGNED LLC RESONANT CONVERTER

Item	Value
Input voltage ( $V_{in}$ )	400V
Output voltage ( $V_o$ )	50V
Output power ( $P_o$ )	800W*2
Resonant inductor ( $L_r$ )	20uH
Magnetizing inductance ( $L_m$ )	110uH
Resonant capacitor ( $C_r$ )	54nF
Transformer turns ratio ( $N_1:N_2$ )	4:1
Quality factor (Q)	0.45

**Interleaved resonant converter controller:** The gate pulses with a phase difference of 90 degree are required for the interleaved operation of the two-phase LLC resonant converter.

The circuit of generating the interleaved gate pulses and key waveforms are given in Fig. 5. In Fig. 5, G1 and G2 are the gate signals for the main switch generated from the resonant converter controller. The two gate signals have complementary values with a dead time. The each flip-flop

operates on the rising edge of the gate signal G1 and the falling edge of gate signal G2, respectively, and generates outputs Q1 and Q2. The third and fourth flip-flops operate on the rising edge of gate signal G2 and the falling edge of gate signal G1 and generate outputs Q3 and Q4, respectively. In Fig. 5, the gate signal G11 of the upper switch of the first converter can be obtained through the logical AND of Q1 and Q2, and the gate signal G12 of the lower switch can be obtained through the logical NOR of Q1 and Q2. The gate signals for driving the second converter can also be implemented in the same manner using pulses Q3 and Q4. This logic circuit generates the phase-shifted gate pulses with 90 degrees (G11 and G21, G12 and G22). The proposed gate pulse generating circuit is simple and easy to implement without the hardware burden.

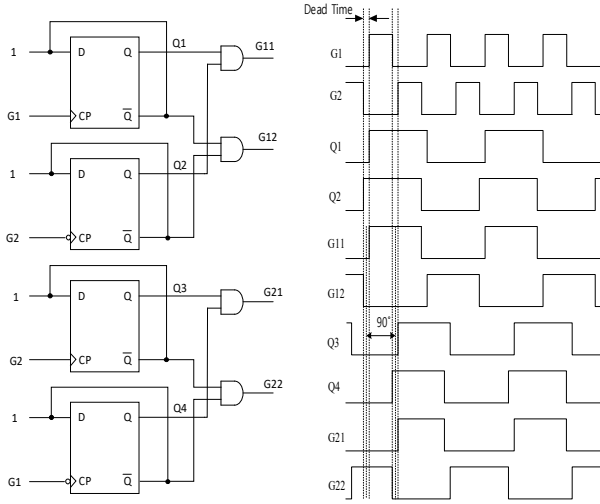


Fig. 5. Interleaved gate pulse generation circuit and waveforms.

The current balancing of two converters is another important issue for the control of the interleaved LLC resonant converter [6]. The primary currents of both converter modules are measured using the voltage of the resonant capacitors and their maximum values are limited by the current limit circuit. The output voltage and current are also limited for the over voltage and over current protections as shown in Fig. 6. The current limiting circuit consists of a shunt resistor, current sensor, comparator, and photo coupler for isolation. The voltage and current limits are selected with an appropriate margin for the output voltage and output current. If the value of the voltage and current applied to the comparator is higher than the reference, a fault signal is generated and this signal biases the primary side transistor through the photo coupler. This signal is applied to the pin that determines the threshold voltage of the analog resonant controller and blocks the main input voltage to stop the operation of the circuit. The value at which the current is blocked is shown in equation (5). The hardware design including the transformer and PCB is also important to balance the impedance of the current paths for both converters.

$$V_{out,max} = I_{out,max} \cdot R_{sense} \cdot Gain \quad (5)$$

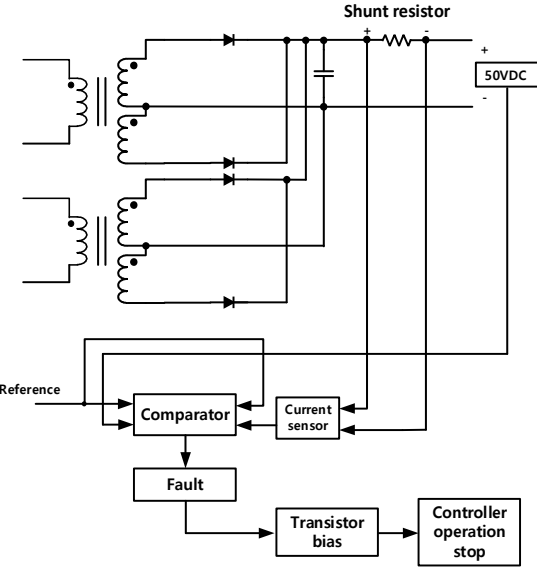


Fig. 6. Structure of voltage and current limiting circuit.

where  $V_{out,max}$  and  $I_{out,max}$  are the maximum output voltage and maximum output current, respectively,  $R_{sense}$  is the value sensed by the shunt resistor.

**Integrated magnetic transformer:** The size reduction of the magnetic components is very important issue for increasing the power density of the LLC resonant converters [7]. The integrated magnetics (IM) planar transformer is proposed to implement the inductor and transformer for the resonant tank using a single ferrite core.

The resonant inductor integrated in the transformer is implemented by inserting a magnetic sheet between the primary and secondary PCB windings, the structure of the IM planar transformer using a leakage layer technique are described in Fig. 7

The magnetic sheet ( $\mu_r = 230$ ) is inserted in the leakage layer between the primary and secondary PCB windings to intentionally increase the leakage inductance. The series resonant inductor can be implemented using the leakage inductance without any additional windings. The measured magnetizing and leakage inductances of the implemented transformers are  $L_m = 110\mu H$ ,  $L_r = 20\mu H$ . Fig. 8 shows the photograph of the implemented integrate magnetic planar transformer.

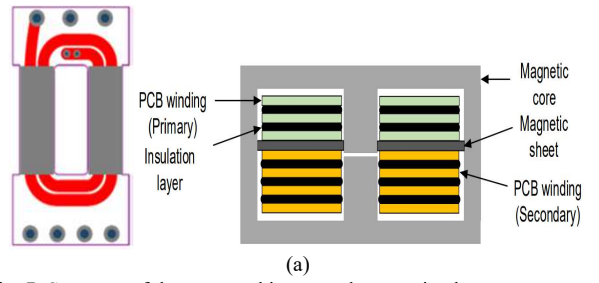


Fig. 7. Structure of the proposed integrated magnetic planar transformer

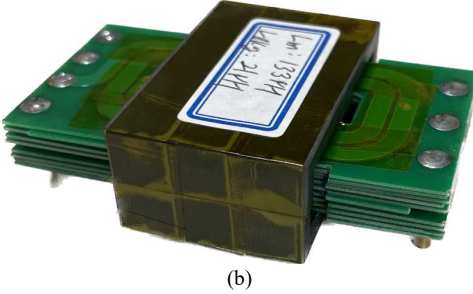


Fig. 8. Photograph of implemented integrated magnetic planar transformer.

### III. EXPERIMENTAL RESULTS

The proposed on-board power supply is implemented for the experimental verification. The photograph of the implemented power supply is shown in Fig. 9, where the two-phase interleaved LLC resonant converter of a power rating of 1.6kW (800Wx2), auxiliary DC-DC converter and power source swapping circuit are included in this system. The used devices for the on-board power supply are as:

- MOSFET: IPDD60R105CFD7 (Infineon)
- Rectifier Diode: RB238NS150FH (Rohm)
- Resonant controller: ICE2HS01G (Infineon)



Fig. 8. Photograph of proposed on-board power supply.

The experimental works rea carried out for the implemented power supply to verify the design. Figs. 10, 11 and 12 show the experimental waveforms of the implemented converter for 20%, 50% and 100% load conditions, where the gate pulses, primary side currents, secondary rectified currents of each converter module, and output voltage are shown.

It is shown in these figures that the implemented two-phase LLC resonant converter is well operated with the interleaved control for various load conditions. Fig. 13 shows the thermal image of the implemented conventional transformer and IM planar transformer under the full load condition. The maximum temperature at the hot spot is measured as 73.4°C, 53.9°C respectively, and it is shown in Fig. 13 that the operation of the IM transformer and converter is thermally stable under the full load condition. The efficiency of the proposed converter using the IM planar transformer was measured and compared with the

efficiency of the conventional LLC resonant converter using an external resonant inductor as shown in Fig. 14.

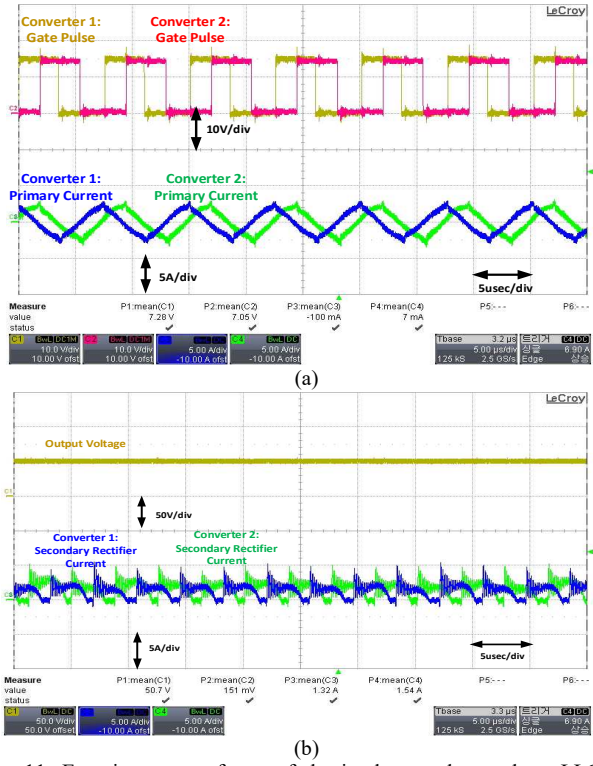


Fig. 11. Experiment waveforms of the implemented two-phase LLC resonant converter for 20% load. (a) Phase shifted gate signal and primary current. (b) Output voltage and secondary rectifier current.

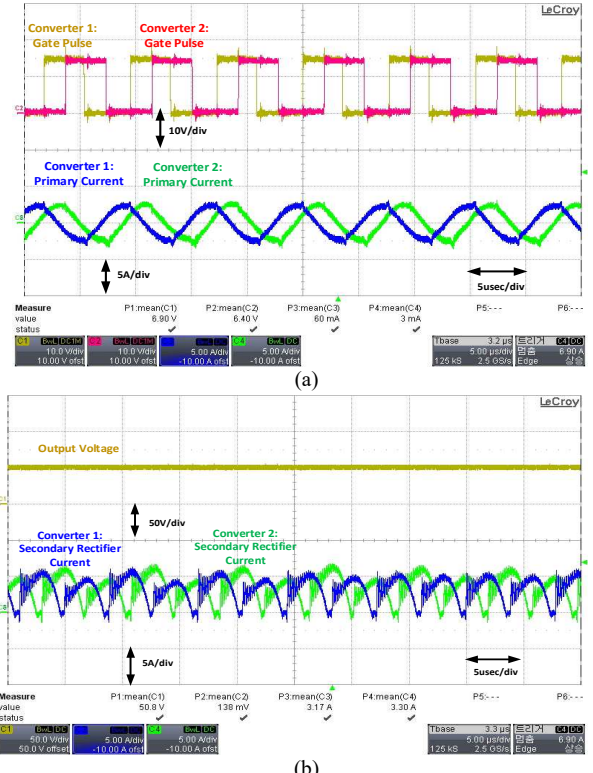


Fig. 12. Experiment waveforms of the implemented two-phase LLC resonant converter for 50% load. (a) Phase shifted gate signal and primary current. (b) Output voltage and secondary rectifier current

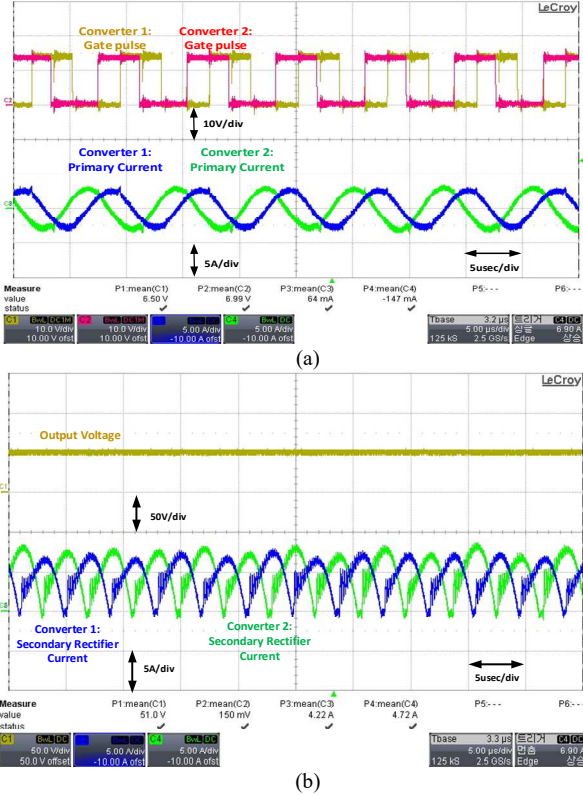


Fig. 12. Experiment waveforms of the implemented two-phase LLC resonant converter for 100% load. (a) Phase shifted gate signal and primary current. (b) Output voltage and secondary rectifier current.

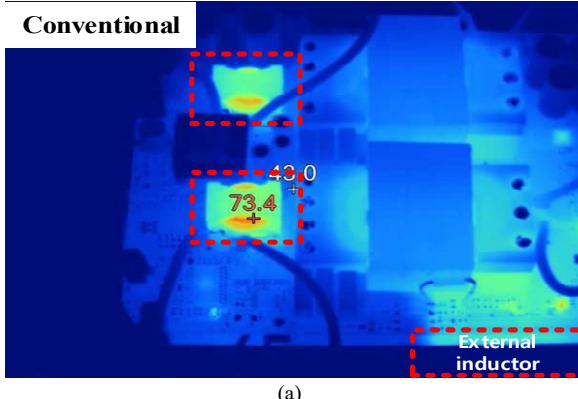


Fig. 10. (a) Thermal image of conventional transformer. (b) Thermal image of IM planar transformer.

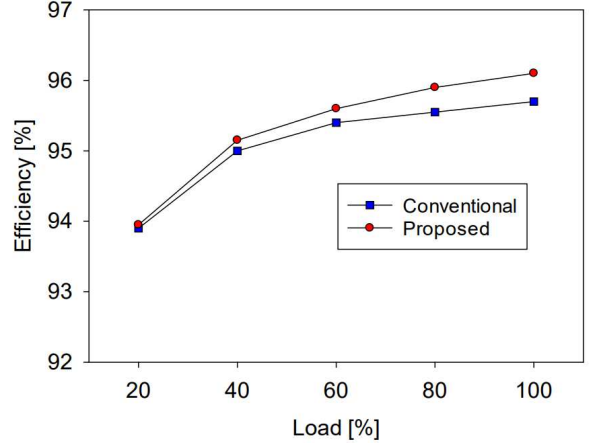


Fig. 11. Measured efficiencies of the conventional and proposed converters.

The maximum efficiency of the proposed converter is 96.1% at the full load condition. It is shown in this figure that the efficiencies of the proposed converters are slightly higher than those of the conventional converters because the elimination of the external inductor.

#### IV. CONCLUSIONS

The design of an on-board power supply for the tether drone applications were presented. The interleaved LLC resonant converter was considered for the main topology, and the design of the converter circuit and implementation of the IM planar transformer were presented. The proposed techniques were applied for the two-phase interleaved LLC resonant converter with a power rating of 1.6kW and the input/output voltages of 400V/50V. When using the proposed integrated transformer, the volume of the magnetic component could be reduced by 11.5%, and the power density was calculated to be 328W/in<sup>3</sup> and 376W/in<sup>3</sup> respectively in the existing and proposed methods. The experimental results showed that the maximum efficiency is 96.1% at the full load condition and is higher than that of the conventional converter with the external inductor.

#### ACKNOWLEDGMENT

This work was supported by the Ministry of SMEs and Startups (S3195753).

#### REFERENCES

- [1] Elistair, Orion 2 Tethered UAS. [Online]. Available: <http://www.elistair.com>
- [2] M. D. P. Emilio, "Tethered Drones for Unlimited Flight Time," EE Times Europe, Jan. 15, 2021. [Online]. Available: <https://eetimes.eu/tethered-drones-for-unlimited-flight-time>
- [3] M. N. Boukoberine, Z. Zhou and M. Benbouzid, "Power supply architectures for drones - A review," in Proc., IEEE IECON 2019, Lisbon, Portugal, Oct. 2019, pp. 5826-5831.
- [4] W. Walendziuk, D. Oldziej and M. Slowik, "Power supply system analysis for tethered drones application," in Proc., Int. Conf. Mechatronic Syst. and Materials, Bialystok, Portugal, July. 2020, pp. 1-6.

- [5] K.-H. Yi and G.-W. Moon, "Novel two-phase interleaved LLC series-resonant converter using a phase of the resonant capacitor," *IEEE Trans. Ind. Electron.*, vol. 56, no. 5, pp. 1815-1819, May 2009.
- [6] B. R. Lin, P. L. Chen and C. L. Huang, "Analysis of LLC converter with series-parallel connection," *2010 5th IEEE Conference on Industrial Electronics and Applications*, Taichung, Taiwan, 2010, pp. 346-351.
- [7] H. Chen, X. Wu and S. Shao, "A current-sharing method for interleaved high-frequency LLC converter with partial energy processing," *IEEE Trans. Power. Electron.*, vol. 67, no. 2, pp. 1498-1507, February 2020.
- [8] Hu, Zhiyuan, et al. "An interleaved LLC resonant converter operating at constant switching frequency." *IEEE Transactions on Power Electronics* 29.6 (2013): 2931-2943.
- [9] C. Fei, R. Gadelrab, Q. Li, and F. C. Lee "High-frequency three-phase interleaved LLC resonant converter with GaN devices and integrated planar magnetics," *IEEE Jour. of Emerg. Select. Topics on Power electron*, vol. 7, no. 2, pp. 653-663, June 2019.
- [10] HUANG, Hong. Designing an LLC resonant half-bridge power converter. In: 2010 Texas Instruments Power Supply Design Seminar, SEM1900, 2010. p. 2010-2011.
- [11] De Simone, S., et al. "Design-oriented steady-state analysis of LLC resonant converters based on FHA." *International Symposium on Power Electronics, Electrical Drives, Automation and Motion, 2006. SPEEDAM 2006.. IEEE*, 2006.
- [12] King, R., and T. A. Stuart. "A normalized model for the half-bridge series resonant converter." *IEEE Transactions on Aerospace and Electronic Systems* 2 (1981): 190-198.